

Density functional theory study of the electronic structure of fluorite Cu₂Se

Mikael Råsander,^{1,*} Lars Bergqvist,^{1,2} and Anna Delin^{1,2,3}

¹*Department of Materials Science and Engineering,*

Brinellväg 23 KTH (Royal Institute of Technology), SE-100 44 Stockholm, Sweden

²*SeRC (Swedish e-Science Research Center), KTH, SE-100 44 Stockholm, Sweden*

³*Department of Physics and Astronomy, Uppsala University, Box 516, SE-751 20 Uppsala, Sweden*

(Dated: December 3, 2024)

We have investigated the electronic structure of fluorite Cu₂Se using density functional theory calculations within the LDA, PBE and AM05 approximations as well as with the non-local hybrid PBE0 and HSE approximations. Our results show that Cu₂Se is a zero gap semiconductor when using either a local or semi-local density functional approximation while there exists a gap when using the PBE0 functional. For the HSE approximation, we find that the presence of a gap depends on the range separation for the non-local exchange within the HSE approximation. For the occupied states we find that the LDA, PBE, AM05, PBE0 and HSE agrees when regarding the overall structure, however, the hybrid functionals are shifted towards lower energy values compared to the LDA, PBE and AM05. The valence bands obtained using the hybrid functionals are in good agreement with experimental valence band spectra. We also find that the PBE, PBE0 and HSE approximations give similar results regarding bulk properties, such as lattice constants and bulk modulus. In addition, we have investigated the localization of the Cu d-states and its effect on the band gap in the material using the LDA+U approach. We find that a gap is opened up by increasing the U , however, the U values required for a gap opening is unrealistically high.

I. INTRODUCTION

The copper chalcogenides Cu₂X (X = S, Se, and Te) are of possible technological interest because of their thermo- and photoelectric properties as well as ionic conductivity. Cu_{2-x}Se, which is the focus of this study, has in particular received attention due to a high ionic conductivity, with possible applications in solar cells^{1,2} as well as a good material for thermoelectric converters.³ At room temperature Cu_{2-x}Se is a rather good p-type conductor with an optical band gap of 1.23 eV.⁴ The Cu_{2-x}Se system has a rather complicated atomic structure where the phase diagram consist of two phases: The low temperature α -phase and the high temperature β -phase.⁵ The β -phase with the space group Fm $\bar{3}$ m has the Se atoms in a face-centered cubic (fcc) environment while the superionic Cu atoms are randomly distributed on interstitial positions in the structure, where the majority of the Cu ions are positioned close to the tetrahedral interstitial sites.^{6,7} The low temperature phase is stable up to about 400 K and has a lower symmetry crystal structure, where the Cu atoms are localized. We point out that the α to β transition varies with the stoichiometry and for $x = 0.15 - 0.25$ the high temperature phase is stable at room temperature.⁸ In addition, we note that both the high and the low temperature phases can be imagined as deviations from the fluorite crystal structure with the difference lying in the occupation of the tetrahedral interstitial positions.

Recently Liu et al.³ showed that Cu_{2-x}Se exhibited excellent thermoelectric properties for a bulk material with a thermoelectric figure of merit of 1.5 at 1000 K. The reasons for the favorable thermoelectric properties were a low thermal conductivity due to the quasi-liquid behavior of the superionic Cu atoms as well as due to a rather

high value of the power factor, i.e. $S^2\sigma$ where S is the Seebeck coefficient and σ is the electrical conductivity.³ It is interesting that a material with a very simple chemical formula, such as Cu_{2-x}Se, has such a low thermal conductivity since this is usually reported for complex systems containing heavy elements, such as doped skutterudites and clathrates, or in nanostructures.⁹ Further investigations of the physical properties of Cu_{2-x}Se as well as other similar systems are therefore important in order to obtain a fundamental understanding of the thermoelectric properties of the Cu_{2-x}Se system in particular and superionic solids in general. In this paper we will present results obtained by density functional theory calculations on the electronic structure of Cu₂Se. The aim with the present study is to obtain a theoretical understanding of the electronic structure of Cu₂Se by means of density functional theory (DFT) calculations in order to establish the accuracy and applicability of various approximations for the exchange-correlation energy (XC) functional within DFT.

The paper is arranged as follows: In Section II we will present the necessary details of our calculations, in Section III we will present our results and in Section IV we will summarize our results and draw conclusions.

II. DETAILS OF THE CALCULATIONS

We have performed density functional theory calculations for Cu₂Se in the fluorite structure, space group Fm $\bar{3}$ m, shown in Fig. 1. This structure is an idealized version of the high temperature phase of Cu₂Se and serves as a good model for determining the accuracy of various approximations for the XC functional. As is shown in Fig. 1, the fluorite structures has the Se

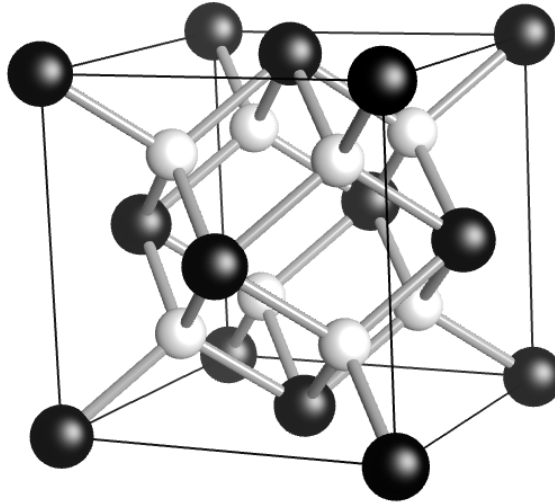


FIG. 1. The crystal structure of fluorite Cu_2Se where Cu atoms are depicted by small (white) spheres and Se by large (black) spheres. The Cu-Se bonds are shown in grey.

atoms positioned at a regular fcc crystal lattice while the Cu atoms occupies the tetrahedral interstitial positions in the fcc lattice.

The Kohn-Sham equation has been solved using Blöchl's projector augmented wave method¹² as it is implemented in the Vienna *ab initio* simulation package (VASP).^{13,14} Calculations have been performed using the local density approximation (LDA), the generalized gradient approximation of Perdew, Burke and Ernzerhof (PBE)¹⁷ as well as with the AM05 functional of Armiento and Mattsson.^{18–20} Since local and semi-local approximations to the XC functional are known to perform badly when determining the band gaps of semiconductors and insulators we have in addition performed calculations with the more advanced hybrid functionals of Perdew, Ernzerhof and Burke (PBE0)²¹ and of Heyd, Scuseria and Ernzerhof (HSE).^{22,23} These functionals have been found to be an improvement of the LDA and PBE when regarding for example bond distances and dissociation energies in molecules as well as structures and band gaps of bulk materials.^{22–25} Interestingly, the AM05 has been found to yield the same level of accuracy as the hybrid functionals when regarding bulk properties of crystals, such as lattice constants and bulk modulus.¹⁹

The PBE0 and HSE are non-local hybrid theories where the exchange part of the exchange-correlation functional includes some non-local contribution. In the PBE0 approximation the XC energy can be expressed by

$$E_{xc}^{PBE0} = \frac{1}{4}E_x^{HF} + \frac{3}{4}E_x^{PBE} + E_c^{PBE}, \quad (1)$$

where E_x^{PBE} and E_c^{PBE} are the exchange and correlation terms in the PBE approximation and E_x^{HF} is the Hartree-Fock exchange energy. In the HSE approximation the XC

energy is given by^{22,23}

$$E_{xc}^{HSE} = E_x^{HSE} + E_c^{HSE}, \quad (2)$$

where

$$\begin{aligned} E_x^{HSE} = & \alpha E_x^{HF,SR}(\omega) + (1 - \alpha) E_x^{PBE,SR}(\omega) \\ & + E_x^{PBE,LR}(\omega), \end{aligned} \quad (3)$$

where *LR* and *SR* denote long range and short range parts respectively, α is a mixing parameter governing the strength of the non-local exchange and ω is a screening parameter that controls the spatial range over which the non-local exchange part is important. The correlation energy in the HSE approximation, E_c^{HSE} , is taken to be identical to the PBE correlation energy as in the PBE0 approximation. The amount of Hartree-Fock exchange in the HSE is the same as in the PBE0, i.e. $\alpha = 1/4$, while the range separation parameter, ω , has to be determined by comparison with experimental data. It has been found that $\omega = 0.2 - 0.3 \text{ \AA}^{-1}$ give good results regarding structural as well as electronic properties of materials, with $\omega = 0.2 \text{ \AA}^{-1}$ being the optimum choice.^{22–24} Unless otherwise specified, $\omega = 0.2 \text{ \AA}^{-1}$ has been used in the HSE calculations. We note that for $\omega = 0$ Eq. (2) is equivalent to the PBE0 and, furthermore, Eq. (2) asymptotically reaches the PBE for $\omega \rightarrow \infty$.²² We will return to this point in Sec. III.

An issue with the use of common density functional approximations is the description of strongly localized orbitals such as d- and f-orbitals. For this reason we have also investigated how the localization of the Cu 3d-states affects the electronic structure as well as the band gap in the system by employing the use of an on-site Coulomb interaction within the LDA+U approximation, using the approach of Dudarev et al.²⁶ We note that in the Dudarev et al. approach the on-site Coulomb interaction, U , and on-site exchange interaction, J , do not enter separately but only in the combination of an "effective U", $U_{eff} = U - J$. However, throughout the presentation we will simply refer to the "effective U" as U . The U has been applied solely to the Cu 3d states.

For the main part of the calculations, the plane wave basis set was cut-off at 1000 eV and we have used a k-point mesh of $30 \times 30 \times 30^{15}$ for the primitive cell of Cu_2Se . However, since the hybrid functionals are much more computationally cumbersome than the local and semi-local approximations, we have used a plane wave cut-off of 800 eV and a k-mesh of $10 \times 10 \times 10$ in combination with the hybrid functionals.

The pseudopotential (PP) for Cu has the 3d and 4s electron states treated in the valence while the semi-core 3s and 3p states have been placed in the core of the PP. For Se the PP has the 4s and 4p electron states treated as valence states.

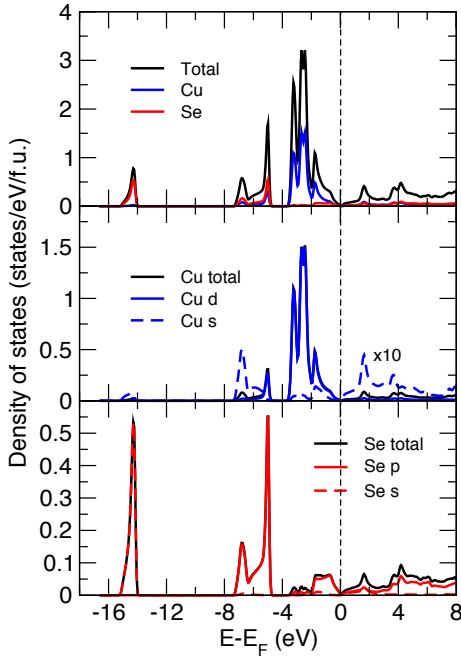


FIG. 2. (Color online) Calculated density of states and projected density of states obtained by using the PBE. The upper panel is the total DOS (black) and the DOS projected on the Cu and Se atoms. The middle panels is the projected Cu DOS with Cu 3d- and 4s-states marked. The lower panel is the projected Se DOS with Se 4p- and 4s-states marked. The vertical dashed line marks the position of the Fermi level E_F . In the middle panel the DOS for the Cu 4s-states has been magnified 10 times.

III. RESULTS

The lattice constants and bulk modulus obtained using the various functionals are summarized in Table I. We note that the PBE, PBE0 and HSE functionals give very similar results in good agreement with experimental observations. The lattice constants are within 1.4 % larger compared to the experimental value with the PBE being the approximation that deviates more. The LDA differs from the other three functionals with a lattice constant that is smaller than the experiment with about 1.7 %, as well as a greater bulk modulus than the PBE and hybrid functionals, which is a consequence of the overbinding of the LDA. The AM05 is the functional that are closest to the experimental lattice constant where the deviation is less than 1 %. When adding the on-site Coulomb interaction, U , to the LDA we find that the lattice constants decreases with an increased U . The bulk modulus is also becoming more similar to the PBE and the hybrid approximations as U increases. Usually, the application of an on-site interaction is expected to increase the lattice constant since the U reduces the kinetic energy of the electrons by allowing them to lower their energy by localization. This leads to a lessened binding energy for the electrons for which a U has been applied and in turn

TABLE I. Calculated bulk properties of fluorite Cu_2Se obtained using the LDA, PBE, AM05, PBE0 and HSE approximations for the XC functional. a is the lattice constant and B is the bulk modulus. The lattice constants and bulk modulus are evaluated using a Birch-Murnaghan 3rd order equation of state.²⁸ The lattice constants and bulk modulus in the second and third columns correspond to the XC functional in the first column while the fifth and sixth columns correspond to the U given in the fourth column within the LDA+U approximation.

XC functional	a (Å)	B (GPa)	U (eV)	a (Å)	B (GPa)
LDA	5.661	111			
PBE	5.844	82	2	5.650	108
PBE0	5.833	81	4	5.637	105
HSE	5.838	80	6	5.623	103
AM05	5.722	97	8	5.605	100
			10	5.583	98
			12	5.554	97
Exp.	5.759 ²⁷				

an increase in the lattice constant. A reduced lattice constant may although appear since the population of strongly bonding s- or p-states may increase on the account of the d-states which results in an increased binding strength.

In Fig. 2, we show the electron density of states (DOS) as evaluated using the PBE functional. It is clear from the results in Fig. 2, that the valence band consists of three regions, a lower region between 14 eV and 15 eV below the Fermi level, which solely is built up by Se 4s-states, a middle region in-between 5 eV and 7.5 eV below the Fermi level that is a mixture of states derived from both Cu and Se, and an upper region from the Fermi level down to 3.5 eV that mostly consists of Cu 3d-states even though there are mixing with the Se 4p-states. We note that there is a Cu 3d peak in the DOS at about 3 eV below the Fermi level that is positioned in-between two regions of Cu 3d and Se 4p hybridized regions, the lower region between about -8 eV to -5 eV and the upper region from about -2 eV to the Fermi level. This behavior of a Cu 3d peak centered in-between regions of hybridized Cu 3d and Se 4p states has been found experimentally by Domashevskaya et al.,²⁹ even though the exact positions of the peaks differs which we will turn to shortly. We also note that the result presented in Fig. 2 is in agreement with the previous tight binding calculation of Garba and Jacobs¹⁰ as well as with the LDA result of Kashida et al.¹¹ A notable result is that the PBE functional yield a zero gap between the occupied valence bands and the unoccupied conduction bands. As was mentioned in Section I, optical studies have reported a band gap of 1.23 eV.⁴ This is a rather small gap and density functional theory is known to underestimate the band gap of semiconductors and insulators when using local and semi-local approximations. In order to investigate the band gap for this system further we will have to resort to more complex approximations to the exchange-

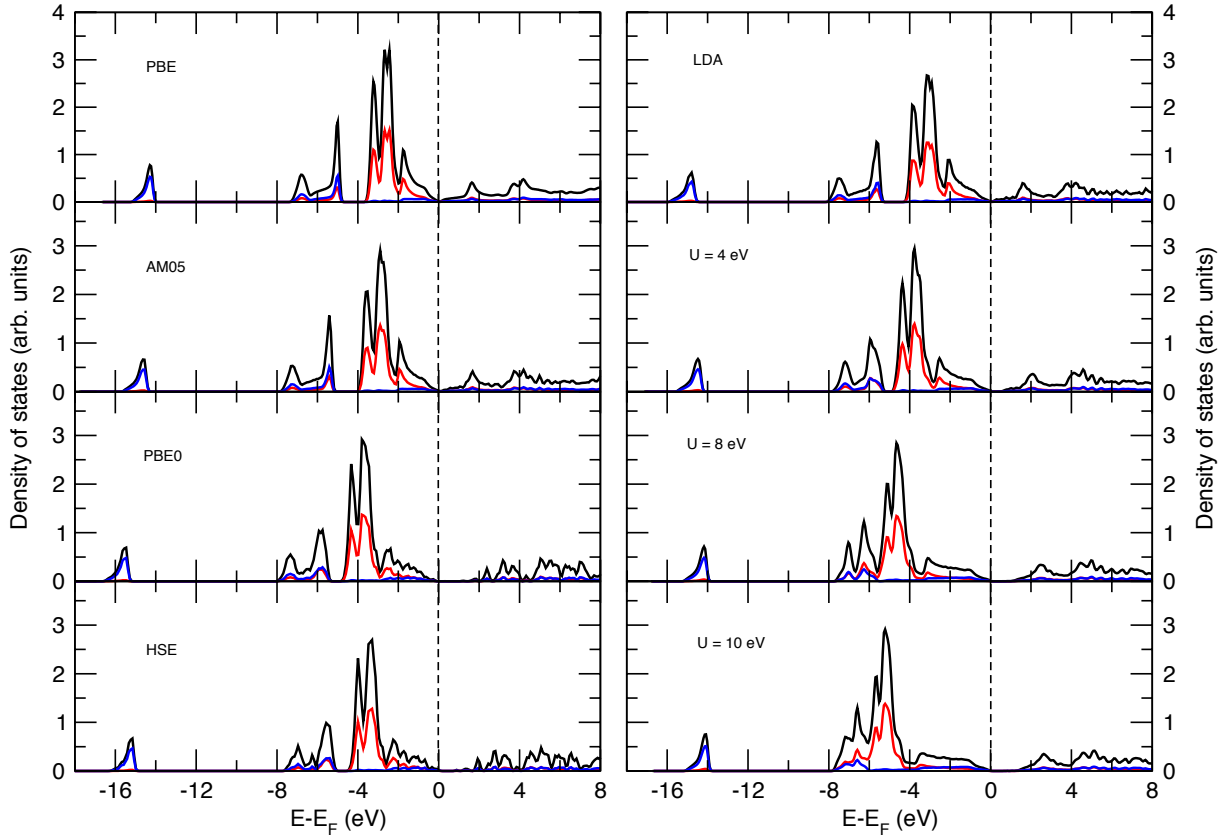


FIG. 3. (Color online) Calculated density of states for PBE, AM05, PBE0 and HSE in the left column and for LDA and LDA+U, with $U = 4$ eV, 8 eV and 10 eV, in the right column. The vertical dashed lines marks the position of the Fermi level E_F for each case. The total DOS is shown in black and we also show the projected DOS on the two different atomic species; Cu in red and Se in blue.

correlation functional.

In Fig. 3 we compare the DOS obtained using the LDA, PBE, AM05, PBE0 and HSE as well as LDA+U. We find that the overall shape of the DOS is very similar to the PBE, which was discussed previously, except for when very large U -values have been applied, and the valence states can be divided into lower, middle and upper valence regions, even though the energies of the states are different. Compared to the PBE the predominant trend is a shift of the states towards lower energies. For the LDA and AM05 this shift is rather small. For the PBE0 and HSE we find that the lower valence region is found between 15 eV and 16 eV below the Fermi level, compared to 14 eV to 15 eV for the PBE. The middle valence region is also shifted downwards with the same amount (~ 1 eV). For the upper valence region the lower edge is shifted downwards with about 1 eV for the hybrid functionals. For very large U the upper valence states is shifted more than the states in the middle valence region and for $U = 8$ eV and 10 eV the upper and middle valence regions from the PBE description have merged into a single region. We note that the valence band DOS obtained by the PBE0 and the HSE functionals are in very good agreement with the x-ray photoelectron spec-

troscopy (XPS) presented by Kashida et al.¹¹ and Domashevskaya et al.²⁹ who found that the main peak in the XPS, which were derived from Cu 3d states, where positioned at 3.5 eV binding energy which is excellently described by the main Cu peak obtained in the DOS from the PBE0 and the HSE approximations as well as for $U = 4$ eV, see Fig. 3. For larger U -values the Cu d-states are found at lower energies than the experimental result. The LDA, PBE and AM05 have the Cu d-states at slightly to high energy compared to the experiment.

When regarding the conduction bands and especially the band gap, we find that all approximations have a region of rather small DOS above the Fermi level, especially the hybrid functionals as well as large U calculations yield a very small DOS in the region from the Fermi level up to about 2 eV. This could mistakenly be taken as a band gap of the same order, however, band gaps should always be evaluated from band structure calculations and not from the DOS where smearing effects could affect the size of the evaluated band gaps.

Figure 4 shows the calculated band structure for the upper valence band as well as for a few conduction bands along high symmetry directions in the Brillouin zone. As is clear, only the PBE0 and LDA+U ($U = 10$ eV) re-

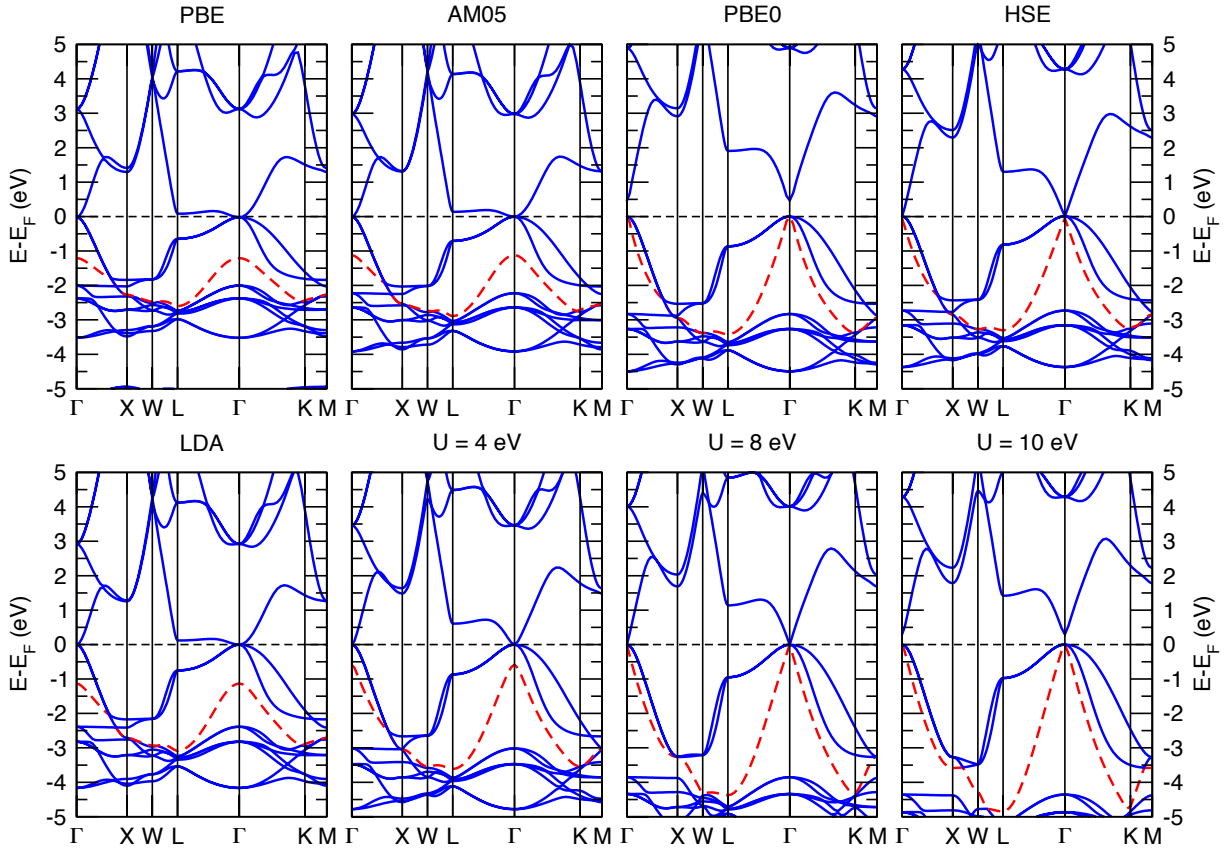


FIG. 4. (Color online) Calculated band structures along directions of high symmetry in the Brillouin zone for Cu₂Se obtained using the LDA, PBE, AM05, PBE0 and HSE functionals. The vertical solid lines label high symmetry coordinates while the horizontal dashed line marks the position of the Fermi level, E_F . Note the common feature that in order for a gap to be open the HOMO-2 band, marked by the (red) dashed band, has to reach the Fermi level, which only happen in the case of the PBE0 and LDA+U with $U=10$ eV.

veals a band gap. In all other cases the highest occupied molecular orbital (HOMO) and the lowest unoccupied molecular orbital (LUMO) touch at the Γ -point. The LDA, PBE and AM05, has an almost flat conduction band along the Λ line (Γ to L), where the LUMO at L is only ~ 0.1 eV above the Fermi level. For these functionals the lowest conduction band are degenerate with two valence bands at Γ . The same is also true for the HSE approximation as well as for $U = 4$ eV and 8 eV. However, as can be seen in Fig. 4, the HOMO-2 band at the Γ -point is very different in the HSE compared to the PBE. This band has moved up towards the Fermi level in the HSE and is found at 0.07 eV below the Fermi level compared to the PBE where this band is found at 1.19 eV below the Fermi level. For the PBE0 this band has moved up to the Fermi level and the HOMO at the Γ -point is triply degenerate with a direct gap of 0.47 eV. The same situation is the case for $U = 10$ eV but the gap is 0.30 eV.

When an on-site Coulomb exchange is added to the Cu 3d states, the main effect is that the Cu 3d states are pushed further down below the Fermi level as witnessed by the projected DOS in Fig. 3. We find that the upper

valence bands in Fig. 4 is becoming broader and the conduction bands are shifted towards higher energies. The major effect is a shift in the low-lying conduction band along the Λ -line (Γ and L). In order for a gap to be open very large U -values are required. The lower right panel of Fig. 4 shows the resulting band structure with $U = 10$ eV. The behavior of the valence and conduction bands with $U = 10$ eV is rather similar to the PBE0 results in the Fermi level near region, i.e. about -2 eV to 2 eV, with a direct band gap at Γ of similar size as the PBE0. We find that the HOMO-2 band is key for the formation of a band gap within the LDA+U approximation. At $U = 8$ eV, this band just reaches the Fermi level and marks a transition situation and a small increase of the Coulomb exchange interaction to 8.1 eV (not shown) gives a small gap at Γ .

Common features of the band structures shown in Fig. 4 are that the highest valence band, as well as the lowest conduction band, is found along the Λ line and that the ordering of the bands are similar irrespective of the approximation that has been used. We also note that the valence band obtained by the PBE0 and HSE approximations are very similar, as is also witnessed by the DOS

TABLE II. Calculated transitions between HOMO and LUMO levels at high symmetry points in the Brillouin zone. Energies are given in eV. The values given within parenthesis for the HSE is obtained by adding the PBE0 band gap of 0.47 eV to the conduction band of the HSE.

$\Delta\epsilon$	PBE	AM05	PBE0	HSE	LDA	$U = 4$ eV	$U = 8$ eV	$U = 10$ eV
$\Gamma \rightarrow \Gamma$	0.00	0.00	0.47	0.00 (0.47)	0.00	0.00	0.00	0.30
$\Gamma \rightarrow L$	0.10	0.14	1.91	1.29 (1.76)	0.12	0.61	1.14	1.42
$\Gamma \rightarrow X$	1.31	1.31	2.91	2.28 (2.75)	1.26	1.49	1.69	1.78
$L \rightarrow \Gamma$	0.63	0.70	1.33	0.82 (1.29)	0.75	0.86	0.95	1.27
$L \rightarrow L$	0.73	0.85	2.77	2.11 (2.58)	0.87	1.47	2.09	2.39
$L \rightarrow X$	1.94	2.02	3.78	3.11 (3.58)	2.01	2.35	2.64	2.76
$X \rightarrow \Gamma$	1.82	2.03	3.00	2.44 (2.91)	2.17	2.66	3.25	3.57
$X \rightarrow L$	1.92	2.17	4.44	3.73 (4.20)	2.29	3.27	4.39	4.69
$X \rightarrow X$	3.13	3.34	5.45	4.73 (5.20)	3.43	4.15	4.94	5.05

in Fig. 3. The difference between these two hybrid approximations lies in the obtained conduction bands where the conduction bands in the PBE0 are found higher above the Fermi level compared to the HSE. The band structure data shown in Fig. 4 are quantified in Table II where we show the evaluated energy differences between HOMO and LUMO levels at various high symmetry points in the Brillouin zone. We note that the difference between the PBE0 and the HSE approximations does not lie in a rigid shift of the conduction bands since by adding the PBE0 band gap of 0.47 eV to the HSE energy differences yield a better agreement between these two approximations, however, some of the transition energies shown in Table II are still off the PBE0 result by as much as 0.2 eV for several transitions.

Since the PBE0 and HSE calculations yield very sim-

ilar valence bands but significantly differ regarding the position of the conduction bands it is important to analyze the difference between these two approximations and in Fig. 5 we show the calculated band gaps obtained by varying the range separation parameter within the HSE approximation, ω . The standard values for this parameter is within the range of 0.2-0.3 Å⁻¹ and $\omega = 0.2$ Å⁻¹ is considered to be the optimum choice.²²⁻²⁴ We find that by going below the optimized ω window a gap opens up, which reaches the PBE0 value at $\omega = 0$. The reason for this behavior can be linked to the neglect in the HSE approximation of the long range contributions of the Hartree-Fock and PBE contributions to the exchange energy, see Ref. 22. By expressing the PBE0 expression in Eq. (1) in short and long range parts along the lines of the HSE approximation²² we find that

$$E_{xc}^{PBE0} - E_{xc}^{HSE} = \alpha (E_x^{HF,LR}(\omega) - E_x^{PBE,LR}(\omega)), \quad (4)$$

where α is the amount of Hartree-Fock exchange that is included (1/4 in the present case). It is therefore not surprising that the PBE0 and HSE approximations do not yield the same results unless the two terms on the right hand side of Eq. (4) either cancel or that both are identically zero. And that by varying ω it is possible to bring the HSE result in closer agreement with the PBE0.

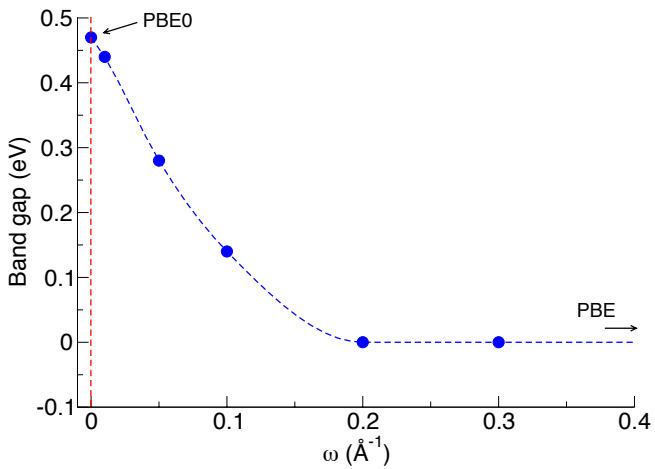


FIG. 5. (Color online) Evaluated band gaps using various values for the range separation parameter ω within the HSE approximation. Note that $\omega = 0$ in the figure is the PBE0 result. Furthermore, as $\omega \rightarrow \infty$ the PBE result is obtained. The points for $\omega = 0.01, 0.05, 0.1$, and 0.3 Å⁻¹ have been evaluated using the lattice constant obtained with $\omega = 0.2$ Å⁻¹ and the points are connected by a fitted spline. The vertical dashed line marks $\omega = 0$.

IV. SUMMARY AND CONCLUSIONS

We have performed density functional theory calculations of the electronic structure of fluorite Cu₂Se using a variety of approximations for the XC energy functional. We find that the PBE, PBE0 and HSE approximations give very similar results regarding lattice constants and bulk modulus. The overall electronic structure of the occupied valence states obtained is rather similar between the different approximations, however, the hybrid functionals PBE0 and HSE are the ones that agrees the best with experimental valence band spectra where the agreement is excellent. In addition, we find that the only approximations that yield a non zero band gap is the PBE0

approximation as well as within the LDA+U approximation where a significant value for the on-site Coulomb exchange interaction is required for a gap to open.

In comparison to experimental band gaps we conclude that the present calculations do not reproduce the obtained optical gap of 1.23 eV obtained by Sorokin et al.⁴, however, this can be due to several reason where one is related to the structure of the system. It is possible that defects, most likely Cu vacancies or interstitials, affects the electronic structure in such a way that larger gaps are obtained and further investigations along these lines are under way. We point out that the experiment was performed at room temperature and for the ordered low temperature phase of Cu₂Se which has a lower symmetry than the fluorite structure. For the to Cu₂Se similar chalcogenide Ag₂Te, which also has a low and high temperature phase similar to Cu₂Se, calculations using the GGA has shown a zero gap for the fluorite structure, while a gap was opened for a lower symmetry monoclinic structure phase.³⁰ The same may also be true for Cu₂Se, that a sizeable gap opens for the low temperature phase and that the fluorite structure has a vanishingly small gap. This behavior is also supported by our calculations since it has been found that the HSE with $\omega \sim 0.2 \text{ \AA}^{-1}$ is better at describing the band gap in small gap semiconductors than the PBE0, where the HSE tends to underestimate band gaps while the PBE0 tends to yield too large gaps.²⁴ Furthermore, localization of the Cu 3d-states cannot account for the formation of a gap since this

requires unrealistically large U -values, and compared to experimental valence band spectra large U -values push the Cu 3d-states too low compared to the Fermi level. $U \sim 4 \text{ eV}$, however, agrees rather well with experimental valence spectra and also agrees well with the hybrid functional calculations.

Furthermore, by inspection of Fig. 3 there is a region of very small DOS above the Fermi level which is derived from the single conduction band that drops down at Γ . It is possible that the experimental resolution cannot resolve this region accurately. If good agreement with optical experiments is required it will be necessary to resort to solving the Bethe-Salpeter equation or using time-dependent DFT where optical gaps can be described properly due to the inclusion of the electron-hole interaction in these methods. However, such calculations are not considered by us at present.

V. ACKNOWLEDGEMENTS

This work was financed through the EU project Nextec, VR (the Swedish Research Council), and SSF (Swedish Foundation for Strategic Research). The computations were performed on resources provided by the Swedish National Infrastructure for Computing (SNIC) at the National Supercomputer Centre in Linköping (NSC).

* mikra@kth.se

- ¹ H. Okimura, T. Matsumae, and R. Makabe, *Thin Solid Films*, **71**, 53 (1980).
- ² W. S. Chen, J. M. Stewart, and R. A. Mickelsen, *Appl. Phys. Lett.*, **46**, 1095 (1985).
- ³ H. Liu, X. Shi, F. Xu, L. Zhang, W. Zhang, L. Chen, Q. Li, C. Uher, T. Day and G. J. Snyder, *Nature Mater.*, **11**, 422-425 (2012).
- ⁴ G. P. Sorokin, Y. M. Papshev, and P. T. Oush, *Sov. Phys. Solid State*, **7**, 1810 (1966).
- ⁵ T. B. Massalski, H. Okamoto, P. R. Subramanian, and L. Kacprzak, *Binary alloy phase diagrams*, 2nd Edition (ASM International 1990).
- ⁶ S. A. Danilkin, A. N. Skomorokhov, A. Hoser, H. Fuess, V. Rajevac, N. N. Bickulova, *J. Alloy Compd.*, **361**, 57 (2003).
- ⁷ S. A. Danilkin, M. Avdeev, T. Sakuma, R. Macquart. C. D. Ling, M. Rusina, and Z. Izaola, *Ionics*, **17**, 75 (2011).
- ⁸ N. H. Abrikosov, V. F. Bankina, M. A. Korzhuev, G. K. Demski, and O. A. Teplov, *Sov. Phys. Solid State*, **25**, 1678 (1983).
- ⁹ G. J. Snyder and E. S. Toberer, *Nature Mater.*, **7**, 105-114 (2008).
- ¹⁰ E. J. D. Garba and R. L. Jacobs, *Physica B*, **138**, 253 (1986).
- ¹¹ S. Kashida, W. Shimosaka, M. Mori and D. Yoshimura, *J. Phys. Chem. Solids*, **64**, 2357-2363 (2003).
- ¹² P. E. Blöchl, *Phys. Rev. B*, **50**, 17953 (1994).
- ¹³ G. Kresse and J. Furthmüller, *Phys. Rev. B*, **54**, 11169 (1996).
- ¹⁴ G. Kresse and D. Joubert, *Phys. Rev. B*, **59**, 1758 (1999).
- ¹⁵ H. J. Monkhorst and J. D. Pack, *Phys. Rev. B*, **13**, 5188 (1976).
- ¹⁶ J. P. Perdew and A. Zunger, *Phys. Rev. B*, **23**, 5048 (1981).
- ¹⁷ J. Perdew, K. Burke, and M. Ernzerhof, *Phys. Rev. Lett.*, **77**, 3865 (1996).
- ¹⁸ R. Armiento and A. E. Mattsson, *Phys. Rev. B*, **72**, 085108 (2005).
- ¹⁹ A. E. Mattsson, R. Armiento, J. Paier, G. Kresse, J. M. Wills, and T. R. Mattsson, *J. Chem. Phys.*, **128**, 084714 (2008).
- ²⁰ A. E. Mattsson and R. Armiento, *Phys. Rev. B*, **79**, 155101 (2009).
- ²¹ J. P. Perdew, M. Ernzerhof, and K. Burke, *J. Chem. Phys.*, **105**, 9982 (1996).
- ²² J. Heyd, G. Scuseria, and M. Ernzerhof, *J. Chem. Phys.*, **118**, 8207 (2003).
- ²³ J. Heyd, G. Scuseria, and M. Ernzerhof, *J. Chem. Phys.*, **124**, 219906 (2006).
- ²⁴ Y. Matsushita, K. Nakamura, and A. Oshiyama, *Phys. Rev. B*, **84** 075205 (2011).
- ²⁵ J. Paier, R. Hirschl, M. Marsman, and G. Kresse, *J. Chem. Phys.*, **122** 234102 (2005).
- ²⁶ S. L. Dudarev, G. A. Botton, S. Y. Savrasov, C. J. Humphreys, and A. P. Sutton, *Phys. Rev. B*, **57**, 1505 (1998).

²⁷ R. D. Heyding, Can. J. Chem., **44**, 1233-1236 (1966).

²⁸ F. Birch, Phys. Rev. **71**, (1947).

²⁹ E. P. Domashevskaya, V. V. Gorbachev, V. A. Terekhov, V. M. Kasharov, E. V. Panfilova, and A. V. Shchukarev, J. Electron Spectrosc., **114-116**, 901 (2001).

³⁰ W. Zhang, R. Yu, W. Feng, Y. Yao, H. Weng, X. Dai, and Z. Fang, Phys. Rev. Lett., **106**, 156808 (2011).